

Evidences of Flow Induced Crystallization During Characterized Film Casting Experiments

Gaetano Lamberti and Giuseppe Titomanlio*

Department of Chemical and Food Engineering, University of Salerno
Via Ponte don Melillo, I-84084 Fisciano (SA), Italy
Phone +39089964026, Fax +39089964057, e-mail: glamberti@unisa.it

Summary: Film casting experiments were carried out with an iPP resin supplied by Montell. Width, velocity, temperature, crystallinity and orientation profiles along draw direction were measured, respectively by image analysis (width and velocity), a dedicated infrared pyrometer (temperature) and a FT-IR transmission device (crystallinity and orientation). Temperature history of each particle along the draw direction was determined from velocity and temperature profiles.

Experimental crystallinity distributions along draw direction were compared with crystallinity distributions calculated on the basis of the resin quiescent crystallization kinetics description and particle temperature histories. The comparison gives evidence of a relevant effect of the flow on the crystallization kinetics during the process. The effect is, however, consistent with a thermodynamic crystallization temperature increase of only 3 K.

Introduction

It is known that orientation of macromolecules due to flow leads to an increase of crystallization kinetics for semicrystalline polymers. In particular elongational flow is more effective than shear flow to determine orientation and thus effects on kinetics and morphology of crystallization^[1-2].

A lot of effort has been made also in recent years to investigate the effect of flow on crystallization kinetics. From experimental point of view, researchers attention is mainly focused on highlighting the decrease of crystallization induction time by effect of shear flow under isothermal conditions^[2-4]; thus, pointing out the increase of crystallization kinetics with respect to quiescent behaviour, usually investigated only by means of calorimetry which allows either isothermal tests or slow cooling temperature ramps.

On the other hand during polymer processing operations the material crystallises while it is simultaneously under high cooling rates and under the effect of flow; indeed some attempts to model the complex phenomena taking place during real processes have been presented in recent years^[5]. To our knowledge, literature does not report data of flow induced crystallization evidences in term of crystallinity evolution during a process, while the material under flow experiences non-isothermal histories.

The film casting process is characterized by a flow having mainly elongational character, so the basic idea of this work was to adopt film casting as a “model” experiment for the study of FIC.

Film casting experiments of an iPP resin were carried out in this work adopting a flow rate low enough to attain crystallization in air. The resin adopted for the experiments was previously characterized also in the cooling rate range experienced by the polymer during the process; its behaviour being described by a kinetic model^[6].

Crystallization profiles along the draw direction were detected and the results were compared with predictions of crystallization kinetics under both quiescent conditions and the same cooling histories. To this purpose velocity and temperature distributions along the draw direction were simultaneously detected in order to identify thermo-mechanical histories experienced by the resin during the process.

Material and methods

Material

The resin adopted for the experiments performed in this work is a commercial iPP supplied by Montell (T30G, $M_w = 481000$, $M_n = 75000$, tacticity = 87.6%*mmmm*).

Isothermal and slow cooling-rate tests (up to 1°C/s) were performed on that resin by a DSC apparatus (Perkin Elmer DSC7) and reported in a previous work^[6]. Thin polymer samples held between two copper plates were quenched by water sprays and temperature histories during quenching were measured in the same work by a suitable thermocouple connected to a data acquisition system. Cooling rates up to about 200°C/s were obtained. Crystallinity index of final solidified material was calculated from FT-IR spectra on the basis of the method outlined at the end of this section. Overall quiescent crystallization kinetics of the resins was described by a slight modification of the model proposed by Ziabicki^[7] (Lamberti and Titomanlio^[6]). Model equations and parameters values adopted for the description of crystallization kinetics are summarized below (eqq. 1-5 and Table 1, in quiescent conditions $T_m \equiv T_m^0$).

$$\chi_c(t) = \frac{X_c(t)}{X_{eq}} = 1 - \exp\{-[P(t)]^n\} \quad K(t) = \frac{d}{dt}P(t) \quad K = K_{th}(1 + \dot{T}Z)^{1/n} \quad (1, 2, 3)$$

$$K_{th} = \kappa_1 \frac{T(T_m - T)}{(T_m)^2} \exp\left[-\frac{E_a}{RT}\right] \exp\left[-\kappa_2 \frac{(T_m)^2}{T(T_m - T)}\right] \quad (4)$$

$$Z = -B_{ath} \left| \dot{T} \right|^{A_{ath}} \frac{(T_m)^5}{T(T_m - T)^5} \exp\left[\frac{E_a}{RT}\right] \quad (5)$$

Table 1. Parameters of the quiescent crystallization kinetic model

X_{eq}	0.61	dimensionless	κ_1	$2.778 \cdot 10^6$	1/s
n	3	dimensionless	κ_2	5.871	dimensionless
T_m^0	463.15	K	A_{ath}	1.7721	dimensionless
E_a/R	45570	K	B_{ath}	$3.448 \cdot 10^{-57}$	s

Comparison of model prediction and experimental final film crystallinity of quenched samples solidified under quiescent conditions is reported in Figure 1.

Methods

Cast film extrusion was performed with a laboratory-scale extruder equipped with a take-up unit. Tests were performed adopting two different rectangular dies (having the same width, $L_0 = 0.20$ m, and different thicknesses, $S_0 = 0.0005$ m and $S_0 = 0.0003$ m), two extrusion temperatures (473 K and 493 K) and several values of both extrusion screw r.p.m. and take-up velocity. Distance X between extrusion head and take-up rolls was kept constant ($X = 0.4$ m). All runs and relative relevant measured parameters are reported in Table 2, a schematic representation of the film casting process is in Figure 2. Mass flow rate \dot{m} was measured by extrudate weighing; extrusion velocity $v_x(x=0)$ was calculated from mass flow rate and melt density, evaluated at die temperature; take-up velocity $v_x(x=X)$ was simply evaluated from collected film length.

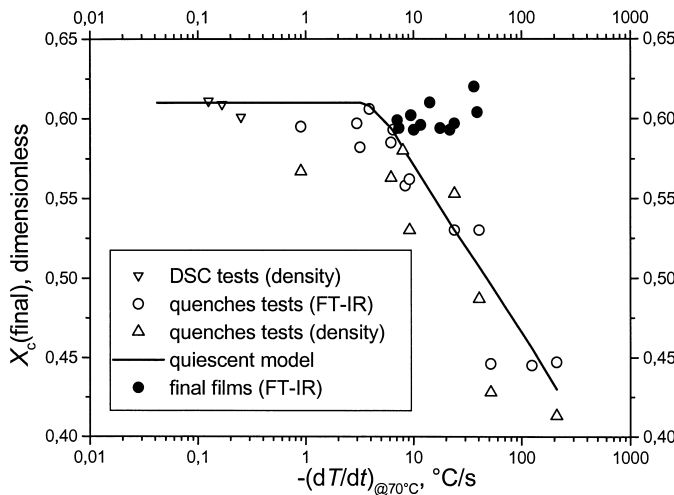


Figure 1. Final crystallinity vs. characteristic cooling rate

Table 2. Operating conditions of the experimental runs

	Ω	\dot{m}	$v_x(x=0)$	$v_x(x=X)$	X	T_0	S_0	$DR = \frac{v_x(x=X)}{v_x(x=0)}$
#	rpm	$10^{-4} \cdot \text{kg} \cdot \text{s}^{-1}$	$10^{-3} \cdot \text{m} \cdot \text{s}^{-1}$	$10^{-3} \cdot \text{m} \cdot \text{s}^{-1}$	m	$^{\circ}\text{C}$	μm	dimensionless
J2	40	2.45	3.25	104.3	0.4	200	500	32.1
J3	30	2.04	2.71	108.3	0.4	200	500	39.9
K1	60	3.39	5.00	58.3	0.4	200	500	11.7
K2	30	1.77	2.35	59.3	0.4	200	500	25.2
K3	20	1.26	1.68	58.3	0.4	200	500	34.7
U1	20	1.33	2.97	71.8	0.4	220	300	24.1
U2	15	1.04	2.33	68.8	0.4	220	300	29.6
U3	12	0.76	1.70	69.7	0.4	220	300	41.1

Width, velocity and temperature profiles along draw direction were measured for all tests. Width distribution along draw direction was obtained by photographic acquisition and subsequent image analysis. In order to avoid any contact with the flowing melt, *on-line* temperature measurements were performed by infrared pyrometry.

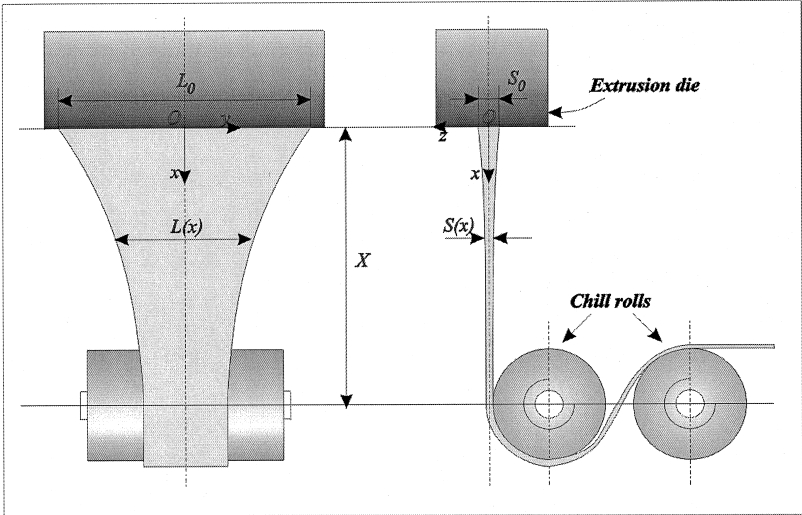


Figure 2. Scheme of the film casting process

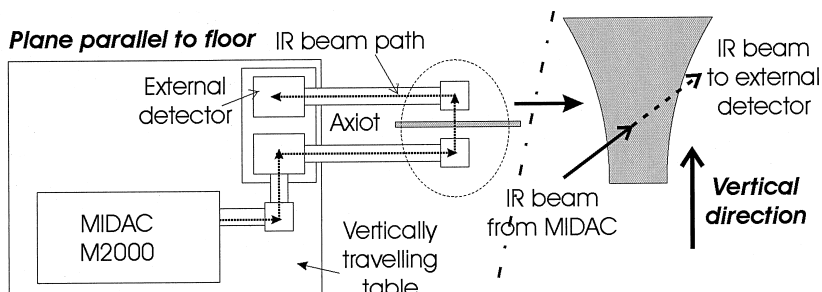


Figure 3. Scheme of the FT-IR spectra collection device

Crystallinity and Hermans orientation factor were determined during the stretching in air by analysis of film FT-IR absorption and of IR dichroism. A M2000 FT-IR spectrometer (by Midac Co.), connected with optical guides (AXIOT, by Axiom Analytical Inc.), was adopted to collect IR spectra *on-line*. The device was mounted on a vertically travelling table. A schematic outline of this device is shown in Figure 3. A typical sequence of absorbance spectra along the draw direction is shown in Figure 4.

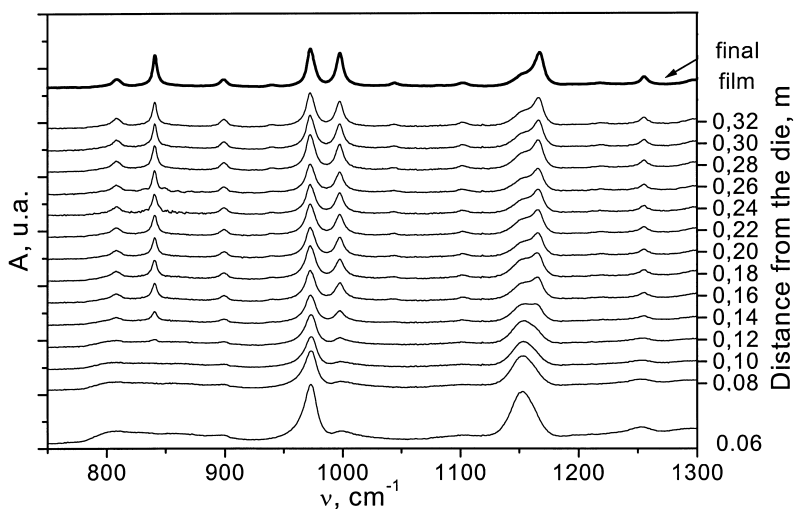


Figure 4. Evolution of absorbance spectra along draw direction

Crystallinity estimation

Crystallinity index was determined by analysis of absorbance of selected peaks of FT-IR spectra, on the basis of Lambert and Beer's law, after peaks assignment. The crystalline

nature of the absorbance peak located at wavenumber of 841 cm^{-1} is well known^[8-11]. After preliminary investigations the absorbance peak at 1153 cm^{-1} was assigned to amorphous phase, and the 973 cm^{-1} absorbance peak was identified as an *internal standard*, i.e. a peak essentially insensitive to amorphous/crystalline ratio^[8, 11]. All the absorbances, here and in the following, were obtained via suitable fitting of experimental spectra. By the way of Lambert and Beer's law, crystallinity index can be written either as:

$$X_c = \frac{A_{841}}{A_{841} + \frac{a_{841}}{a_{1153}} A_{1153}} \quad (6)$$

or

$$X_c = \frac{a_{973}}{a_{841}} \frac{A_{841}}{A_{973}} \quad (7)$$

The ratios $a_{841}/a_{1153} = (1.532)$ and $a_{973}/a_{841} = (0.834)$ were estimated by calibration by means of WAXS diffractograms on quenched samples^[11]. Results obtained from IR spectra by either one of the two equation 6 (based on A_{841} and on A_{1153}) and 7 (based on A_{841} and on A_{973}) are very close to each other, this was taken as a mutual confirmation.

Orientation estimation

Both crystalline phase (f_c) and average (f_{av}) Hermans orientation factors were determined by dichroism. The dichroic ratio at a wavenumber ν is defined as $D_\nu = (A_\pi/A_\sigma)_\nu$, where A_π is the absorbance when polarization plane is parallel to draw direction and A_σ is the absorbance when polarization plane is orthogonal to draw direction. If ν_1 is a wavenumber characteristic of the crystalline phase, Hermans factor of crystalline phase is related to dichroic ratio at ν_1 as:

$$f_c = \left[\left(\frac{D-1}{D+2} \right) \left(\frac{D_0+2}{D_0-1} \right) \right]_{\nu_1} \quad (8)$$

Similarly, if the wavenumber ν_2 is related to a peak sensitive to phase fraction average orientation defined as:

$$f_{av} = f_c X_c + f_{am} (1 - X_c) \quad (9)$$

the average orientation factor is related to dichroic ratio at ν_2 :

$$f_{av} = \left[\left(\frac{D-1}{D+2} \right) \left(\frac{D_0+2}{D_0-1} \right) \right]_{\nu_2} \quad (10)$$

D_{0,ν_1} and D_{0,ν_2} are values of D at total molecular alignment. Procedure outlined above

was first applied to iPP by Samuels [12] with $\nu_1 = 1220 \text{ cm}^{-1}$ and $\nu_2 = 1256 \text{ cm}^{-1}$ ($D_{0,\nu_1} = 2\cot^2(72^\circ) = 0.211$ and $D_{0,\nu_2} = 2\cot^2(38.5^\circ) = 3.161$). With these wavenumbers the procedure applies very well to final products, i.e. the manufactures obtained from the film casting process. Unfortunately the spectra collected *on-line* during the process show a noise higher than the spectra collected *off-line*. As a consequence, the procedure could not be adopted for measurement of f_c by the peaks at wavenumber of 1220 cm^{-1} , its absorbance being of the same magnitude of the background noise signal. Peaks at wavenumber 841 cm^{-1} and the 973 cm^{-1} (the same used in crystallinity measurements) were found much more defined; thus they were calibrated^[11] by means of measurements on final solid films obtaining $D_{0,841} = 2.587$ and $D_{0,973} = 2.546$ and were adopted for the identification of f_c and f_{av} from all collected spectra.

Results and discussion

Width and velocity profiles as measured during the experiments summarized in Table 2, series K and U, are shown in figure 5 below. Extrusion and take-up velocities of the two series were varied in narrow ranges as to obtain similar draw ratios. Thickness of the die is smaller in U series and extrusion temperature is higher for the runs of series U with respect to those of series K. Fitting curves through experimental data are also reported in figure 5.

At some distance from the die, in a position usually called *frozen-line*, the polymer solidifies; downstream from frozen-line both film width and velocity remain essentially constant; density increase causes a small final width and velocity decrease. A criterion to quantify frozen-line position can be to consider the position where width reaches a value 10% higher than the final one.

As for features shown by the curves of width distribution profiles reported in Figure 5, one has to consider that within each of the two series (K and U) the draw ratio was increased by decreasing the flow rate under constant take up velocity. The effect of a decrease of flow rate is two-fold: i) the temperature of the film decreases and the film solidifies more rapidly (i.e. within a shorter distance from the extruder, causing a faster width decrease with distance from the extruder die); ii) final width increases as already pointed out in a previous paper^[13]. As a result a cross over between the curves can take place as observed in the case of series K.

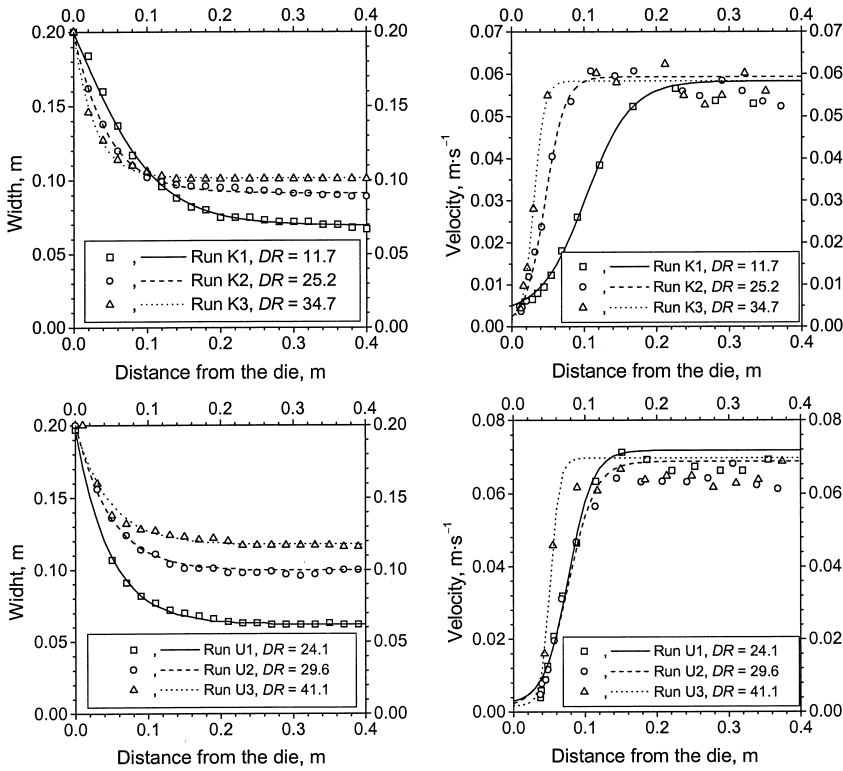


Figure 5. Width and velocity profiles for runs of series K (above) and U (below)
Symbols: experimental; lines: data fitting

Figure 6 shows experimental temperature and crystallinity profiles, during run K1 crystallization took place to close to take up unit to be experimentally detected. Also temperature fitting curves are reported in figure 6. All data show an intermediate plateau in the temperature evolution. Crystallinities were calculated from both eq. 6 (i.e. adopting A_{841} and A_{1153}) and eq. 7 (i.e. adopting A_{841} and A_{973}). The two different methods give results consistent to each other.

Results reported in figure 5 and 6 show a substantial mutual agreement. The plateau mentioned above in the temperature curves have to be related to release of heat of crystallization. Their starting positions always correspond to the position along the drawing direction, where both crystallization starts and frozen line was identified above commenting width and velocity curves. Indeed, this result implies that the polymer resistance to flow dramatically increases by effect of very little crystallinity (a few percent), which was already reported in the literature^[3].

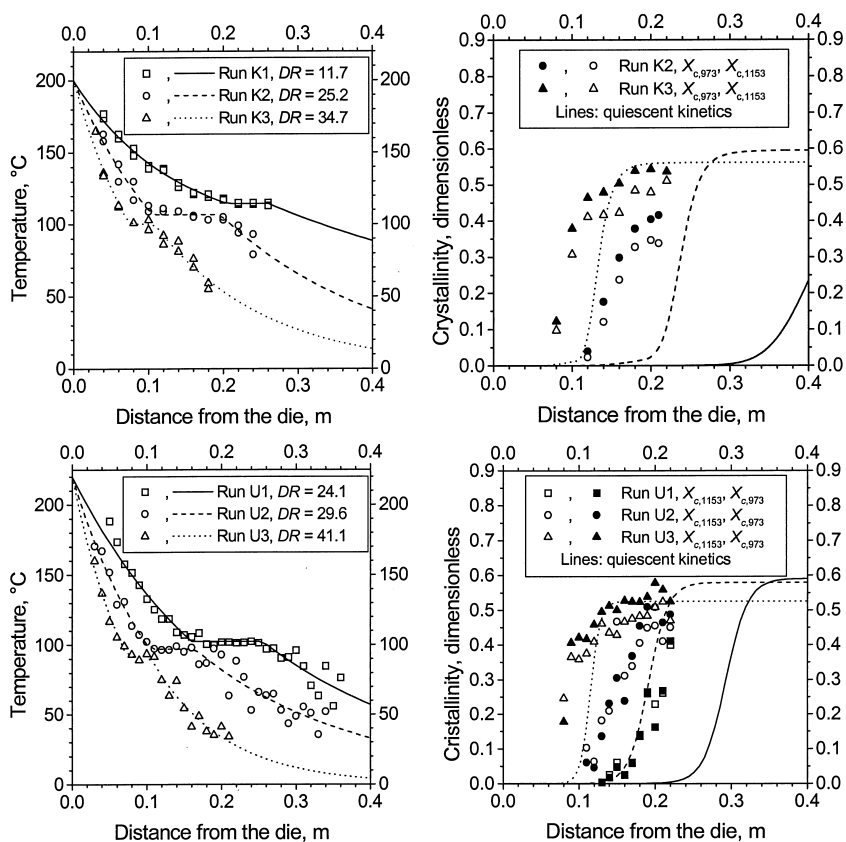


Figure 6. Temperature and crystallinity profiles for series K (above) and U (below) Symbols: experimental data; lines: fitting curves for temperature and predictions of quiescent crystallization kinetics for crystallinity

Cooling history of a material element while moving along the draw direction can be calculated from thermal and velocity profiles by applying the relation:

$$\frac{dT}{dt} = v_x \frac{dT}{dx} \quad (11)$$

Fitting functions showed in figures 5 and 6 were adopted to this purpose. Consistency between crystallinity distributions of Figure 6 detected *on-line* and the quiescent crystallization kinetic model described in the *Material and methods* section can be checked on the basis of cooling histories determined by eq. 11. Crystallinity profiles predicted on the basis of thermal histories and quiescent crystallization kinetic model are compared in Figure 6 with results of *on-line* measurements. The experimental crystallization develops always closer to the extrusion head (and at higher temperatures)

than predicted by the quiescent model.

Temperatures when crystallization reaches one half of its final value, both as measured *on-line* and as calculated from quiescent crystallization kinetics, are reported in Figure 7 for all data as function of cooling rate at 70°C, which Piccarolo *et al.*^[14] suggested as relevant parameter of cooling rates for iPP (also results for J series are reported); indeed, two temperature curves are obtained and both decrease as function of cooling rate at 70°C. Temperatures calculated by the model tuned on quiescent data are about 15°C smaller than those obtained experimentally *on-line*. Such an increase of crystallization temperature is in agreement with results of Göschel *et al.* as reported by Ziabicki^[15].

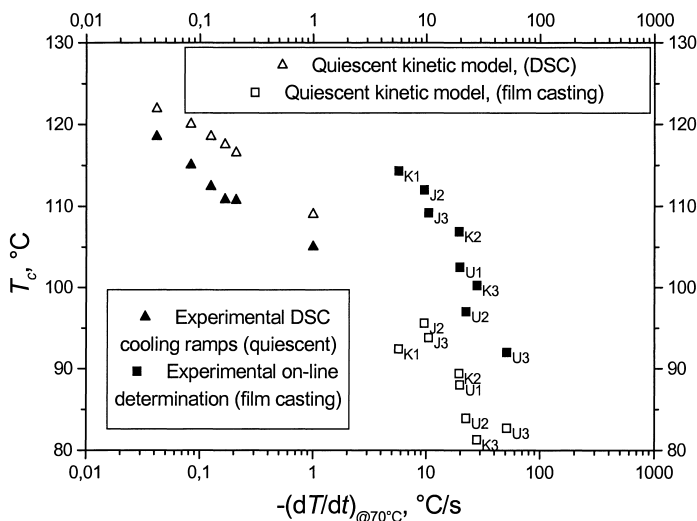


Figure 7. Crystallization temperature vs. characteristic cooling rate

Crystallization temperatures as obtained from calorimetric constant cooling rate ramps and corresponding predictions of quiescent crystallization kinetic model are also reported in the same figure for further validation of the crystallization model. As the comparison shows that the model slightly overpredicts quiescent crystallization temperatures, the 15°C difference between *on-line* crystallization temperatures determinations and predictions of quiescent crystallization model under the same cooling histories have to be related to the enhancement of crystallization kinetics by effect of flow.

Figure 8 displays results of orientation measurements performed *on-line* as function of distance from the extruder die. Crystalline orientation factor (on the left) was directly measured by dichroic ratio D_{841} as specified in *Material and methods* section.

Obviously, crystalline orientation could be measured only where crystallinity was detected. The data show a relevant scatter; however, it is evident that after the onset of crystallization the orientation of crystalline phase is immediately very high. Results of average orientation factor measurements, measured by dichroic ratio D_{973} as specified in *Material and methods* section, are also reported on the right hand side of Figure 8. Orientation of the amorphous phase should be drawn from eq. 9 on the basis of crystallinity and of both average and crystalline orientation factors, the results suffer of the combination of the experimental scatters of each of the three determinations. Values of amorphous orientation have thus an amplified uncertainty, however, they are certainly much smaller than crystalline orientation. Similar observation was already made by Ziabicki^[15] by analysing final products rather than *on-line* measurements and by Lamberti *et al.*^[16] also on final films.

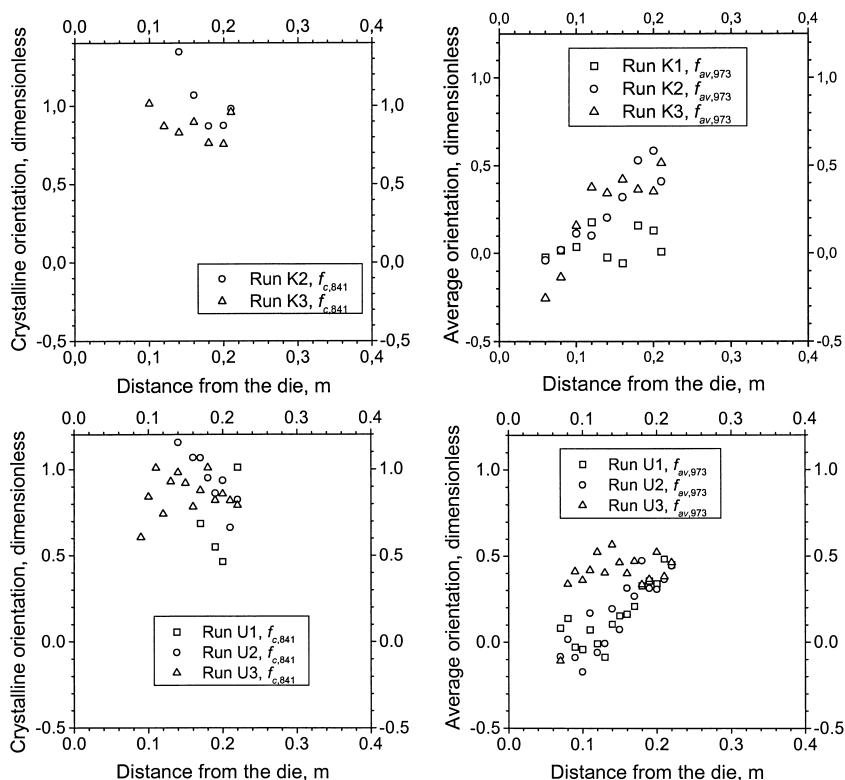


Figure 8. Crystalline and average orientation factor for series K (above) and U (below)

Highly oriented crystallites, thus, form from a slightly oriented melt. This result is a nice confirmation of the very recent Ziabicki's model of selective crystallization of oriented molecules ^[15]. According to this model, even if average orientation in the melt is low, high molecular weight fractions may achieve high orientation by effect of flow and consequently can crystallize at higher temperature giving rise to high crystalline orientation.

Certainly, orientation and some order builds up in the melt by effect of flow, the parallel entropy decrease ΔS^f determines an increase of crystallization temperature according to the well-known relation:

$$T_m = \frac{T_m^0}{1 - T_m^0 \frac{\Delta S^f}{\Delta H}} \quad (12)$$

where T_m^0 is the quiescent melting temperature of the crystals (463 K for iPP in Table 1). The modified melting temperature, T_m as predicted by eq. 12, has to be adopted in kinetic model, i.e. into equations 4 and 5. An increase of melting temperature of only 3-4°C is sufficient to determine an increase of T_c of about 15°C, at the cooling rates experienced by the material during the film casting tests; predictions of kinetics, thus, become very close to experimental *on-line* crystallinity measurements, as Figure 9 shows. Corresponding entropy decrease by effect of flow can be calculated by inversion of eq. 12 as about $3 \text{ J} \cdot \text{kg}^{-1} \cdot \text{K}^{-1}$.

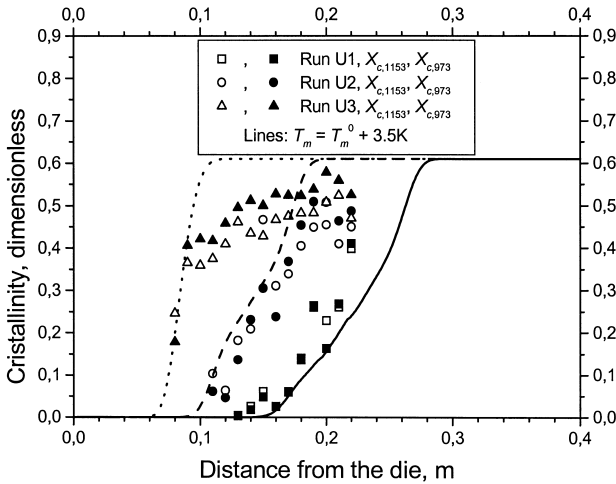


Figure 9. Crystallinity distribution, experimental and predicted with a melting temperature shift of 3.5K

Recently Coppola *et al.*^[4] proposed a method to estimate the free energy change due to flow in a polymeric melt, modeled following reptation theory. This model was adopted for the prediction of induction time during isothermal shear experiments, giving satisfactory results. By applying the equations of that model to our process conditions (which just before film solidification give rise to a deformation rate close to 0.5 s^{-1}) an entropy decrease due to the flow of $3 \text{ J} \cdot \text{kg}^{-1} \cdot \text{K}^{-1}$ is obtained with a relaxation time (T_d) 1.56 s. This value is more than one order of magnitude smaller than the rest relaxation time of the resin adopted in this work as calculated by Coppola *et al.* at the crystallization temperature, while it is of the same order of the material relaxation time under actual deformation rate. If this is not just fortuitous, molecular models of orientation evolution have to be based on values of relaxation time under flowing conditions.

On the other hand, entropy decrease ΔS^f can be related to molecular strain λ on the basis of classical rubber elasticity theory^[17] as

$$\Delta S^f = -\frac{k_B v}{2} \left(\lambda^2 + \frac{2}{\lambda} - 3 \right) \quad (13)$$

where k_B is the Boltzmann constant and v is the number of chain junctions (entanglements for a melt) per volume unit, which is proportional to the inverse of the number of monomer units between two entanglements (60 for iPP, Ferry^[18]). Considering the molecular weight of the resin adopted, quite small values of λ (close to 2) give rise to $\Delta S^f = 3 \text{ J} \cdot \text{kg}^{-1} \cdot \text{K}^{-1}$, the value required to obtain a close description of crystallinity evolution. Indeed, a small value of the molecular strain λ is consistent with the observation made above of a small orientation of the melt at crystallization.

Moreover, as further confirmation of FIC effects, final crystallinity of film casting products (full symbols) is compared in Figure 1 with final crystallinity of manufactures obtained under quiescent conditions, with the same cooling rate. Products obtained under flowing conditions are more crystalline than the others, because of the enhancement effect of the flow on crystallization phenomenon.

Conclusions

Film casting experiments were carried out with an iPP resin and distributions of most relevant variables were measured along drawing direction during the experiments. Thermo-mechanical histories were drawn out from temperature and velocity measurements.

A quiescent kinetic model, tuned by results of both DSC and characterized quenches, was adopted to predict the evolution of crystallinity under quiescent conditions on the basis of thermal histories obtained from the experiments.

Premature crystallization by effect of flow was evidenced by comparing *on-line* experimental results with prediction of the quiescent crystallization model under the same thermal history.

An entropic increase of equilibrium crystallization temperature of about 3 K, when adopted in the quiescent crystallization kinetic model, is sufficient to bring crystallinity prediction very close to experimental data. The same entropic temperature shift is consistent with a small molecular orientation of the crystallizing melt, as found by *on-line* measurements.

Furthermore, crystallinity in final films was found larger than that of samples solidified under quiescent conditions, at same cooling rates. All these results bring clear evidences of flow-induced crystallization.

Acknowledgements

The work is supported by the Italian Ministry of University (PRIN 1999-2001, "Flow induced crystallization of polymers. Impact on processing and manufacturing properties").

- [1] A.J. Pennings, A.M. Kiel, *Kolloid Z.u.Z. Polym.*, **1965**, 205, 160
- [2] R.R. Lagasse, B. Maxwell, *Polym. Eng. Sci.*, **1976**, 16, 189
- [3] G. Titomanlio; V. Speranza, V. Brucato, *Int. Polym. Proc.*, **1997**, XII, 45
- [4] S. Coppola, N. Grizzuti, P.L. Maffettone, *Macromolecules*, **2001**, 34, 5030
- [5] A.K. Doufas, A.J. McHugh, C. Miller, A. Immaneni, *J. Non-Newt. Fluid Mech.*, **2000**, 92, 27; *ibidem*, **2000**, 92, 81
- [6] G. Lamberti, G. Titomanlio, *Polym. Bulletin*, **2001**, 46, 231
- [7] A. Ziabicki, *Colloid Polym. Sci.*, **1996**, 274, 209; *ibidem*, **1996**, 274, 705
- [8] H. Tadokoro, M. Kobayashi, M. Ukita, K. Yasufuku, S. Murahashi, T. Torii, *The Journal of Chemical Physics*, **1965**, 4, 1432
- [9] P.C. Painter, M. Watzek, J.L. Koenig, *Polymer*, **1977**, 18, 1169
- [10] I.M. Ward, *Structure and properties of oriented polymers*, Chapman & Hall, London 1997
- [11] G. Lamberti, R. Crisci, I. Russo, V. Brucato, *Proceedings of XV AIM Annual Meeting*, Trieste, Italy, **2001**
- [12] R.J. Samuels, *Structured polymer properties*, John Wiley & Sons, New York 1974
- [13] G. Lamberti, G. Titomanlio, V. Brucato, *Chem. Eng. Sci.*, **2001**, 56, 5749
- [14] S. Piccarolo, S. Alessi, V. Brucato, G. Titomanlio, in *Crystallization of Polymers*, Ed. M. Dosiè, NATO ASI Series, Kluwer Academic Publisher, **1993**, 475
- [15] A. Ziabicki, *Multidimensional theory of crystal nucleation*, to appear in *Mathematics of polymer processing*, V. Capasso, (Ed.), Springer Verlag, Heidelberg 2002
- [16] G. Lamberti, V. Brucato, G. Titomanlio, *J. Appl. Polymer Sci.*, in press, **2002**
- [17] P.J. Flory, *Principles of Polymer Chemistry*, Cornell University Press, London 1953
- [18] J.D. Ferry, *Viscoelastic Properties of Polymers*, John Wiley & Sons, New York 1980